Photodegradation of Atrazine:
A Comparison of Anatase and Brookite Phases of Titanium Dioxide

Leslie Sigmon
Department of Chemistry
The University of North Carolina at Asheville
One University Heights
Asheville, North Carolina 28804 USA

Faculty Advisor: Dr. Oksana Love

Abstract

Anthropogenic contamination of water resources is one of the most pressing concerns facing our world today. As contaminants trend towards organic, endocrine-disrupting chemicals, generated by agricultural and industrial waste, the need for ever increasing maximum limits on pollutants has surfaced. These new contaminants can pose threats to human health at nearly molecular levels, and nanoparticles, with their diminutive scale, offer a solution to modern water pollution. Photocatalysis and subsequent photodegradation of contaminants using titanium dioxide nanoparticles has been previously investigated, including remediation of atrazine, the most common contaminant in United States drinking water. However, results have been varied and studies have been largely inconclusive, which is likely due to a lack of morphological consistency in titanium dioxide nanoparticles, as well as the restriction of previous studies to anatase-phase titanium dioxide nanoparticles. We propose to synthesize monodisperse brookite-phase titanium dioxide nanoparticles and use them to photodegrade atrazine within a standard photoreactor device. Synthesized particles will be characterized using scanning electron microscopy and X-ray powder diffraction. Their performance will be compared to standard anatase-phase titanium dioxide nanoparticles, and results will be analyzed with UV-visible absorption spectroscopy.

Keywords: Photocatalysis, Atrazine, Brookite

1. Introduction

Securing clean water resources is one of the most pressing tasks of scientists today. Currently, 11% of the global population does not have accessed to improved drinking water sources.[1] The World Health Organization estimates that by 2025, half of the world population will have compromised access to clean water.[2] A rapidly growing threat to global water quality is anthropogenic contamination of the drinking water supply with organic chemicals from pesticides, pharmaceuticals, and industrial solvents.[2,3] In 2001, 5.05 billion metric tons of pesticides were used annually across the world, and agrochemical usage is expected to increase proportionally to the growing global population.[3]

The most commonly used pesticide in the world is atrazine, a broadleaf herbicide.[4] Atrazine functions as a xenoestrogen and has been found to disrupt the endocrine systems and impair the reproductive development of amphibians.[4] It is the most common contaminant in United Stated drinking water, and was banned in the European Union in 2004 due to safety concerns rising from persistent groundwater contamination.[5,6] Atrazine poses a great threat to global drinking water supplies because, although it quickly degrades in soils, once in the water supply it can take many years to degrade into harmless substances.[4,5,6]

Worldwide drinking water quality standards are continually revised to reflect the gains in knowledge of the dangers of atrazine and other organic chemicals, and regulatory agencies continue to decrease the maximum allowable limits of specific contaminants.[3] The efficiency of purification methods must increase, as very low concentrations of these contaminants can be detrimental to human health.[3] As maximum allowable concentration standards approach the molecular level, scientists are looking to nanotechnology for new solutions in water purification.

Photocatalysis is a much studied method for pollution abatement.[7,8] The basic process of photocatalysis is as follows. When a semiconductor catalyst is struck by photons of energy greater than its bandgap, electrons are promoted from the valence band to the conduction band and positively charged holes remain in the valence band.[9] These electron hole pairs are able to effectively degrade organic pollutants into inorganic components through a series of oxidation-reduction reactions.[9] The reaction requires a catalyst with high surface area; nanoscale titanium dioxide (TiO_2), an inexpensive and relatively nontoxic material, is the most commonly used photocatalyst.[8,10-12] TiO_2 exists in three major crystal phases, anatase, rutile, and brookite, of which anatase is the most commonly used in photocatalysis experiments.[7,8,10,11,13]

Photocatalytic degradation of atrazine using TiO_2 has been investigated and many proposed degradation pathways of atrazine can be found in the literature.[14-20] However, the majority of photocatalytic experiments involving TiO_2 have used the widely available Degussa P-25 formulation, which is a mixture of approximately 80% anatase and 20% rutile TiO_2.[8,17-20] Very few studies using the brookite phase have been conducted.[7,11-13] This is likely due to previous difficulties in developing solution-phase synthesis procedures and the lack of availability of pre-prepared brookite nanoparticles for purchase.[7,8,11-13] Of the few brookite studies found in the literature, several have demonstrated that brookite possesses exceptionally good photocatalytic properties, but others have found anatase to be a more effective photocatalyst.[7,8,12,13,21] Very few, if any, brookite studies have focused on the photocatalytic degradation of pesticides.[7,8,11-13]

The objective of this study was to synthesize brookite nanoparticles using the procedure recently described by Gordon, et al. and measure their ability to photocatalytically degrade atrazine.[22] The performance of brookite nanoparticles was compared to that of purchased anatase nanoparticles, with the goal of determining which phase of TiO_2, if any, was more effective at photocatalytic degradation of atrazine.

2. Experimental Methods

Brookite TiO_2 Synthesis. Brookite nanoparticles were synthesized as described by Gordon, et al.[22] The entirety of the procedure was carried out under N_2. In a flask, 10 mL oleylamine, 10 mL 1-octadecene, and 0.48 mL oleic acid were mixed and degassed at 100 °C for 1 hr. A $TiCl_4$ precursor was made, consisting of 0.2 M $TiCl_4$ and 1.0 M oleic acid in 1-octadecene. 1.5 mL of the $TiCl_4$ precursor was added to the flask at 60 °C and then quickly heated to 290 °C and held for 10 min. Another 8 mL $TiCl_4$ precursor was added at approximately 0.3 mL/min, while holding the temperature at 290 °C. The heating mantle was then removed and the flask was allowed to cool to room temperature. Products were rinsed with isopropanol and centrifuged at 8000 rpm for 8 minutes. Supernatant was decanted, and solids rinsed 3 times with isopropanol. Finally, hexane was added to redisperse particles.

$NOBF_4$ Ligand Exchange. The ligand exchange procedure to effect water solubility was adapted from Dong, et al.[23] 0.1 g $NOBF_4$ was dissolved in 10 mL of acetonitrile using sonication. This solution was added to 10 mL of brookite TiO_2 dispersed in hexane. The mixture was sonicated until nanoparticles precipitated and supernatant was discarded.

Characterization of TiO_2. 21 nm anatase TiO_2 nanoparticles were purchased from Aldrich to use for comparison in photocatalytic experiments. Both purchased anatase and synthesized brookite TiO_2 nanoparticles were characterized using scanning electron microscopy (SEM) (FEI Quanta 400) and powder X-ray diffraction (XRD) (Philips PW 3040 Powder X-Ray Diffractometer).

Atrazine Standards. Atrazine standards of concentrations 5000, 4000, 3000, 2000, 1000, and 500 ppb were prepared from atrazine powder purchased from Aldrich. Atrazine standards were characterized with UV-Visible spectroscopy (UV-Vis) (Shimadzu UV-1800 UV-VIS Spectrophotometer).

TiO_2-Atrazine Solutions. 0.0010 g of brookite or anatase TiO_2 was added to 100 mL of each atrazine standard, to make a total of 12 TiO_2-atrazine solutions (6 anatase and 6 brookite TiO_2-atrazine solutions with atrazine concentrations of 5000, 4000, 3000, 2000, 1000, and 500 ppb). TiO_2-atrazine solutions were characterized with UV-Visible spectroscopy (UV-Vis) (Shimadzu UV-1800 UV-VIS Spectrophotometer) before use in photocatalytic experiments.

Photocatalytic Experiments. Approximately 3 mL of TiO_2-atrazine solution in a standard 10 mm quartz cuvette was irradiated at 254 nm using a photoreactor (Rayonet RPR-100 Photochemical Reactor) for a total of 10 min. Cuvette

was removed every 2 min for characterization with UV-Visible spectroscopy (UV-Vis) (Shimadzu UV-1800 UV-VIS Spectrophotometer). This procedure was repeated for all 12 TiO_2-atrazine solutions.

3. Results and Discussion

Fig. 1 shows SEM images of 21 nm anatase TiO_2 purchased from Aldrich (left) and synthesized brookite phase TiO_2 (right). Anatase and brookite nanoparticles appear similar in images. However, the instrument resolution was not sufficient to provide information on particle shape or size. As a result, XRD was used as the primary method for characterization of TiO_2 nanoparticles (Fig.2).
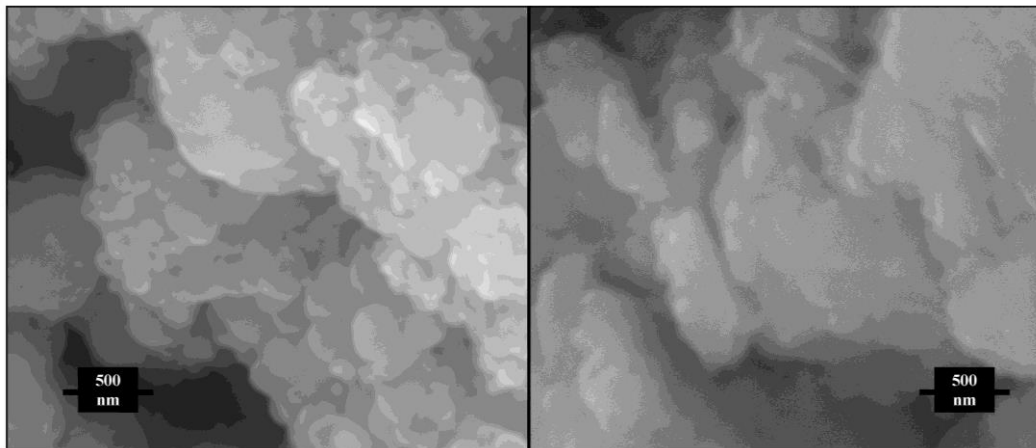
Figure 1. SEM images of anatase TiO_2 (left) and brookite TiO_2 (right).

Powder XRD patterns of anatase and brookite TiO_2 nanoparticles shown in Fig. 2 clearly indicate the crystal phase distinction between the two samples. Anatase data show major peaks corresponding to Miller indices for anatase phase of TiO_2: $2\theta = 25.32°$ {101}, $2\theta = 37.93°$ {004}, $2\theta = 48.32°$ {200}.[24] Major peaks found in the brookite XRD patterns are consistent with Miller indices for brookite phase TiO_2: $2\theta = 25.29°$ {111}, $2\theta = 31.03°$ {121}, $2\theta = 37.97°$ {201}.[8,13,24] The primary difference in XRD patterns for anatase and brookite phases of TiO_2 are at the brookite phase {121} peak, found at $2\theta = 31.03°$ in Fig. 2.[10,11,13,24,25] This peak is absent in anatase phase TiO_2, so XRD data confirm that synthesized particles contain the brookite phase.[11,13,25] Additionally, the appearance of minor peaks at $2\theta = 36.13°$ and $2\theta = 39.43°$, corresponding to the {012} and {022} reflections, further corroborate the presence of the brookite phase.[11,13,25]
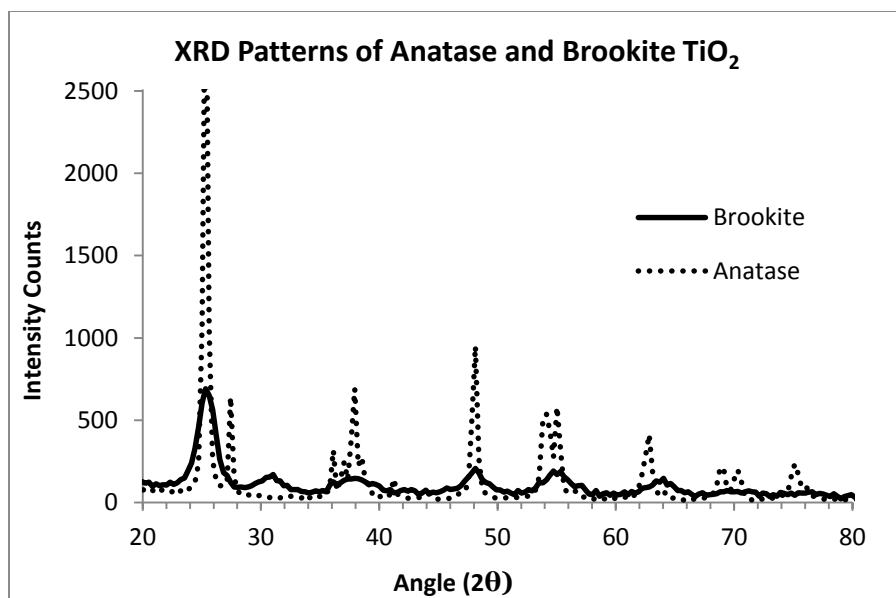
317

Figure 2. Comparison of powder XRD patterns of anatase and brookite TiO_2.

Atrazine standards of concentrations 5000, 4000, 3000, 2000, 1000, and 500 ppb were prepared and analyzed with UV-Vis spectroscopy, as shown in Fig. 3. Although not shown for clarity, absorbances above 490 nm continue horizontally with no additional peaks. The strong absorption peak at 222 nm is characteristic of atrazine, and can be linearly related to atrazine concentration.[17,18] A calibration curve, shown in Fig. 4, plotting absorption at 222 nm against atrazine concentration was prepared and illustrates the use of the concentration-dependent 222 nm absorption peak.[17,18]
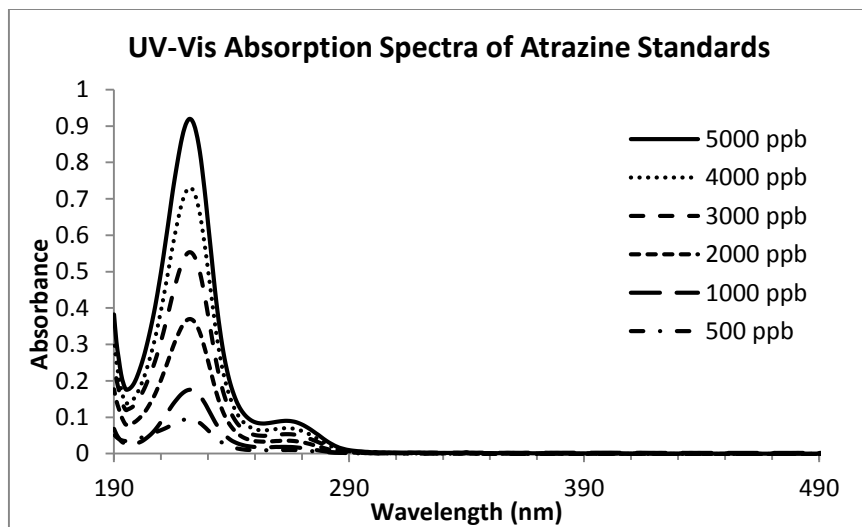

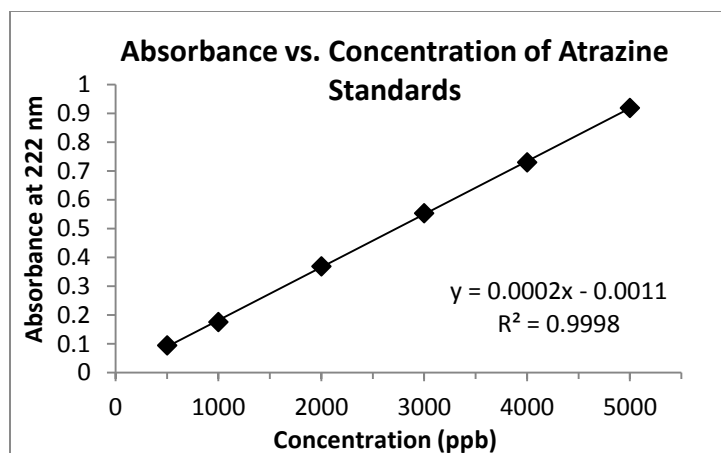Figure 3. UV-Vis absorption spectra for all atrazine standards.

Figure 4. Calibration curve of atrazine standards.

Atrazine standards were mixed with either anatase or brookite TiO_2 and then analyzed with UV-Vis spectroscopy, the results of which are shown in Fig. 5. When compared to the UV-Vis spectra of atrazine standards before mixing with TiO_2 (Fig. 3), the general baseline absorbance as well as the 222 nm peak were inflated due to light scattering. Although not shown for clarity, absorbances above 490 nm continue horizontally with no additional peaks. Fig. 6 shows calibration curves for the TiO_2-atrazine solutions. Variation in TiO_2 mass measurements and light scattering effects contributed a certain amount of variance in the 222 nm peak, leading to increased absorption values and R^2 values lower than those of atrazine standards (Fig. 4). However, the linear relationship between absorbance at 222 nm and concentration of atrazine is still observed in all TiO_2-atrazine solutions and the slope of the regression line is consistent for both atrazine standards and TiO_2-atrazine solutions.
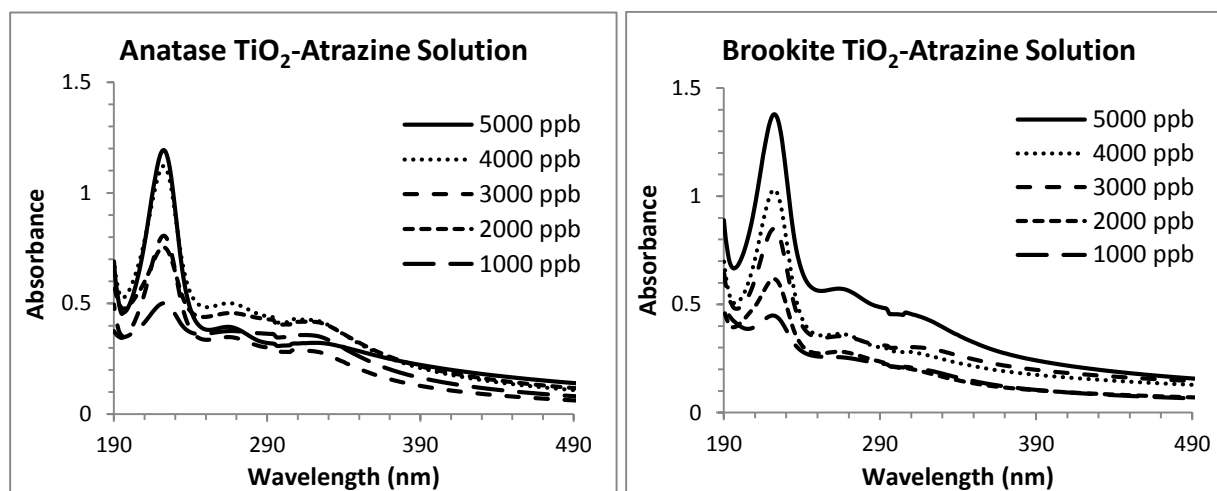

Figure 5. UV-Vis absorption spectra for atrazine standards mixed with anatase (left) and brookite TiO_2 (right).
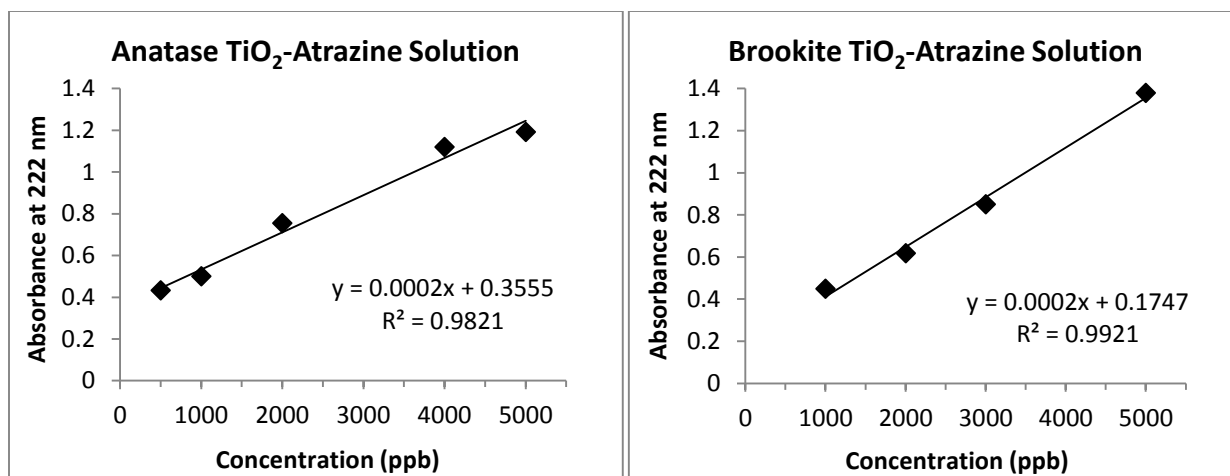
Figure 6. Calibration curve of atrazine standards mixed with anatase (left) and brookite TiO_2 (right).

Fig. 7 shows the change in the UV-Vis absorption spectra of the 3000 ppb atrazine standard mixed with either anatase or brookite TiO_2 after irradiation at 254 nm in the photoreactor. Although not shown for clarity, absorbances above 390 nm continue horizontally with no additional peaks. UV-Vis data were taken every 2 min for 10 min, with the 0 min line representing the TiO_2-atrazine solutions before exposure to irradiation. When mixed with either anatase or brookite, the characteristic atrazine peak at 222 nm quickly degraded and two new peaks at approximately 238 nm and 205 nm were formed. The formation of peaks at these wavelengths in response to irradiation are consistent with previous studies, and correspond to substitution products, like hydroxyatrazine, proposed to form during decomposition of atrazine.[17,19,20] All TiO_2-atrazine solutions followed similar absorption patterns.
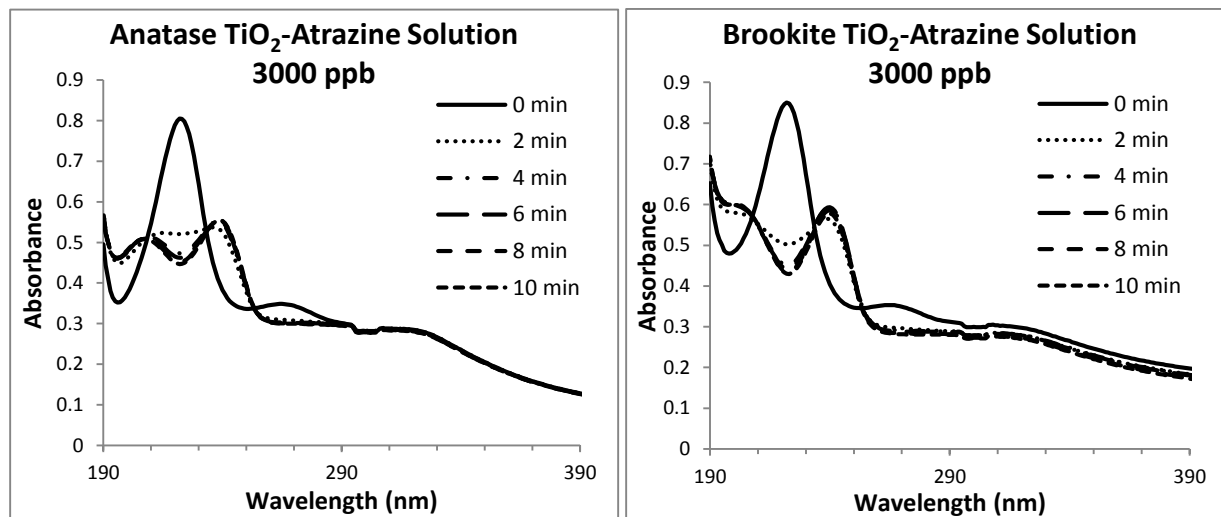

Figure 7. UV-Vis absorption spectra of 3000 ppb atrazine standard mixed with anatase (left) and brookite TiO_2 (right) after 2 min intervals under irradiation in photoreactor.

To acquire the data used in Fig. 8, absorbance values at 222 nm of both anatase and brookite TiO_2-atrazine solutions were collected after every 2 min of irradiation for a total of 10 min and then converted into concentration values via the calibration curves shown in Fig. 6. Data for the 500 ppb TiO_2-atrazine solutions are not shown for clarity. Although the overall increase in absorbance values due to scattering effects in TiO_2-atrazine solutions was somewhat variable, the general trend of atrazine degradation is still quite easily observed. Photocatalyzed anatase and brookite TiO_2-atrazine solutions both showed a large decrease in concentration after the first 2 min of irradiation and the rate of degradation slowed considerably afterwards. However, degradation of atrazine in the brookite TiO_2-atrazine solution within the first 2 min was greater than that of the anatase TiO_2-atrazine solution; when averaged over all atrazine

standards, brookite TiO_2 caused a 10.0 % ± 5.1 % larger decrease in atrazine concentration in the first 2 min as compared to anatase TiO_2. Furthermore, in the final measurement at 10 min of irradiation time, the overall decrease in concentration when averaged over all atrazine standards was 7.7 % ± 7.3 % greater when atrazine was mixed with brookite than with anatase TiO_2.
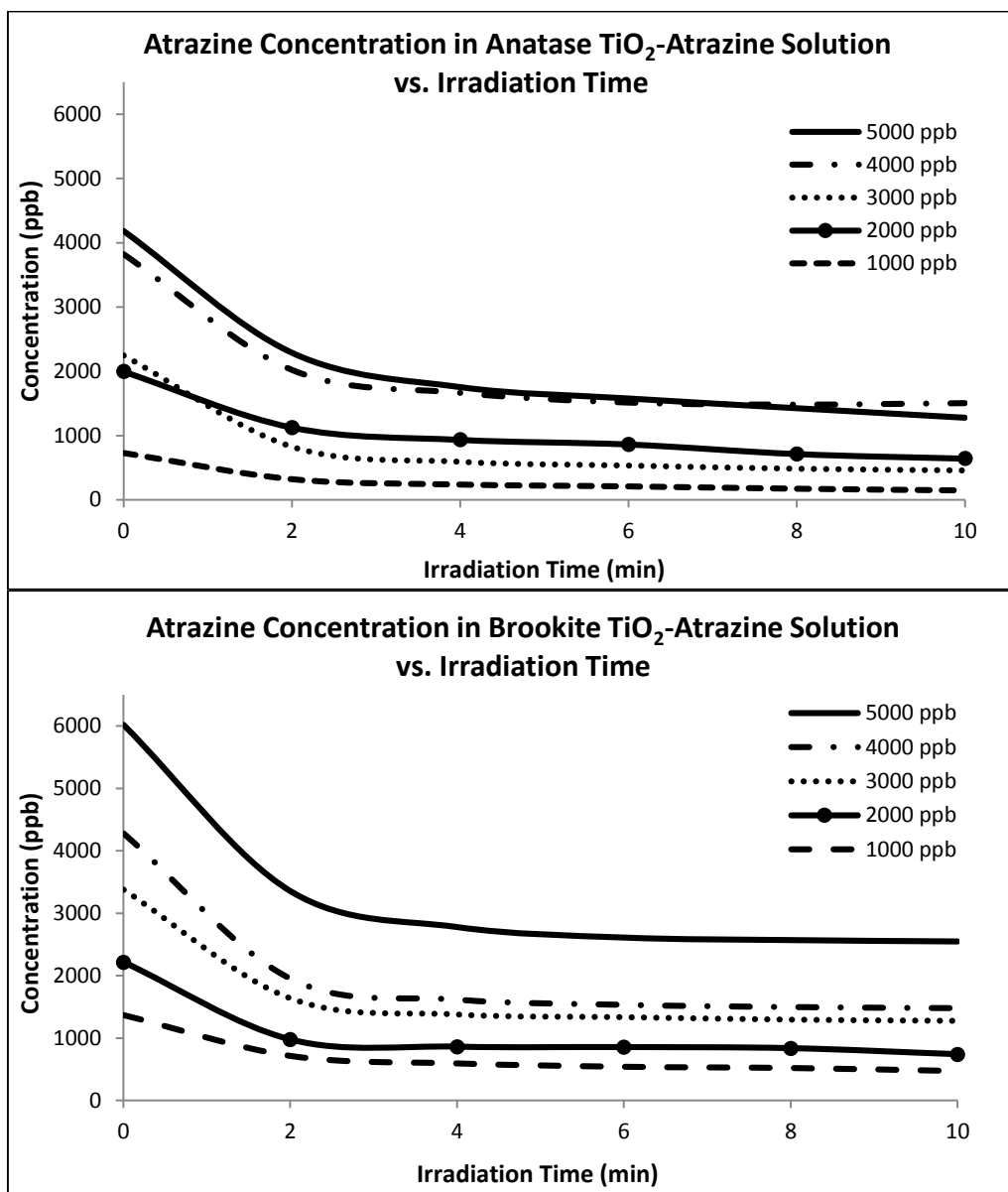

Figure 8. Change in concentration versus irradiation time of atrazine standards mixed with anatase (top) and brookite TiO_2 (bottom).

4. Conclusion

Despite previously reported conflicting data concerning the photocatalytic properties of brookite, the results of this study strongly suggest that brookite phase TiO_2 is a more effective photocatalyst than anatase phase TiO_2 for atrazine degradation. Brookite, when mixed with atrazine, provided a 7.7 % ± 7.3 % greater overall degradation of atrazine than anatase in every sample. Additionally, atrazine degradation within the first 2 min of irradiation was 10.0 % ± 5.1 % greater when atrazine standards were mixed with brookite rather than anatase. Brookite is a promising

photocatalyst and more studies, involving alternative characterization and quantification methods like HPLC or GC/MS, are highly recommended. Nanoscale TiO$_2$, especially the brookite phase, clearly offers potential remediation solutions for water polluted with pesticides and should be further investigated for such use.

5. Acknowledgements

6. References

1. *The Millenium Development Goals Report*. United Nations: New York, 2012. http://www.un.org/millenniumgoals/pdf/MDG%20Report%202012.pdf (accessed 11/09/13).
2. *WHO Water Quality and Health Strategy 2013-2020*. World Health Organization: Geneva, Switzerland, 2013. http://www.who.int/water_sanitation_health/publications/2013/water_quality_strategy.pdf (accessed 11/09/13).
3. Pradeep, T.; Anshup. Noble Metal Nanoparticles for Water Purification: A Critical Review. *Thin Solid Films.* **2009**, *517*, 6441–6478.
4. Hayes, T.; Haston, K.; Tsui, M.; Hoang, A.; Haeffele, C.; Vonk, A. Atrazine-Induced Hermaphroditism at 0.1 ppb in American Leopard Frogs (*Rana pipiens*): Laboratory and Field Evidence. *Environ. Health Perspect.* **2003**, *111*, 568-575.
5. Gilliom, R. J.; Barbash, J. E.; Crawford, C. G.; Hamilton, P. A.; Martin, J. D.; Nakagaki, N.; Nowell, L. H.; Scott, J. C.; Stackelberg, P. E.; Thelin, G. P.; Wolock, D. M. *The Quality of Our Nation's Waters: Pesticides in the Nation's Streams and Ground Water, 1992–2001*; U.S. Geological Survey Circular 1291; U.S. Geological Survey: Reston, Virginia, 2006.
6. L 78/53. *Official journal of the European Union*. Document number C (2004) 731: Brussels, Belgium, 2004.
7. Li, J.; Tang, C.; Li, D.; Haneda, H.; Ishigaki, T. Monodispersed Spherical Particles of Brookite-Type TiO$_2$: Synthesis, Characterization, and Photocatalytic Property. *J. Am. Ceram. Soc.* **2004**, *87*, 1358–1361.
8. Iskandar, F.; Nandiyanto, A. B. D.; Yun, K. M.; Hogan, C. J.; Okuyama, K.; Biswas, P. Enhanced Photocatalytic Performance of Brookite TiO$_2$ Macroporous Particles Prepared by Spray Drying with Colloidal Templating. *Adv. Mater.* **2007**, *19*, 1408–1412.
9. Schneider, J.; Matsuoka, M.; Takeuchi, M.; Zhang, J.; Horiuchi, Y.; Anpo, M.; Bahnemann, D. W. Understanding TiO$_2$ Photocatalysis: Mechanisms and Materials. *Chem. Rev.* **2014**, *114*, 9919−9986.
10. Huberty, J.; Xu, H. Kinetics study on phase transformation from titania polymorph brookite to rutile. *J. Solid State Chem.* **2008**, *181*, 508–514.
11. Koelsch, M.; Cassaignon, S.; Guillemoles, J. F.; Jolivet, J. P. Comparison of optical and electrochemical properties of anatase and brookite TiO$_2$ synthesized by the sol–gel method *Thin Solid Films* **2002**, *403*, 312–319.
12. Kandiel, T. A.; Feldhoff, A.; Robben, L.; Dillert, R.; Bahnemann, D. W. Tailored Titanium Dioxide Nanomaterials: Anatase Nanoparticles and Brookite Nanorods as Highly Active Photocatalysts. *Chem. Mater.* **2010**, *22*, 2050–2060.
13. Kominami, H.; Ishii, Y.; Kohno, M.; Konishi,S.; Kera, Y.; Ohtani, B. Nanocrystalline brookite-type titanium(IV) oxide photocatalysts prepared by a solvothermal method: correlation between their physical properties and photocatalytic activities. *Catal. Lett.* **2003**, *91*, 41-47.
14. Gawlik, B. M.; Moroni, A.; Bellobono, I. R.; Muntau, H. W. Soil Adsorption Behavior and Photomineralization by Photocatalytic Membranes Immobilizing Titanium Dioxide of Atrazine and Intermediates. *Global Nest: the Int. J.* **1999**, *1*, 23-32.
15. Konstantinou, I. K.; Sakellarides, T. M.; Sakkas, V. A.; Albanis, T. A. Photocatalytic Degradation of Selected *s*-Triazine Herbicides and Organophosphorus Insecticides over Aqueous TiO$_2$ Suspensions. *Environ. Sci. Technol.* **2001**, *35*, 398-405.
16. Bellobono, I. R.; Barni, B.; Gianturco, F. Pre-Industrial Experience in Advanced Oxidation and Integral Photodegradation of Organics in Potable Waters and Waste Waters by PHOTOPERM^{TM} Membranes Immobilizing Titanium Dioxide and Promoting Photocatalysts. *J. Membr. Sci.* **1995**, *102*, 139-147.

17. Azenha, M. E. D. G.; Burrows, H. D.; Canle, M.; Coimbra, R.; Fernández, M. I.; García, M. V.; Peiteado, M. A.; Santaballa, J. A. Kinetic and mechanistic aspects of the direct photodegradation of atrazine, atraton, ametryn and 2-hydroxyatrazine by 254 nm light in aqueous solution. *J. Phys. Org. Chem.* **2003**, *16*, 498–503.

18. Mamián, M.; Torres, W.; Larmat, F. E. Electrochemical Degradation of Atrazine in Aqueous Solution at a Platinum Electrode. *Portugaliae Electrochimica Acta* **2009**, *27*, 371-379.

19. Pelizzetti, E.; Maurino, V.; Minero, C.; Carlin, V.; Tosato, M. L.; Pramauro, E.; Zerbinati, O. Photocatalytic Degradation of Atrazine and Other *s*-Triazine Herbicides. *Environ. Sci. Technol.* **1990**, *24*, 1559-1565.

20. McMurray, T. A.; Dunlop, P. S. M.; Byrne, J. A. The photocatalytic degradation of atrazine on nanoparticulate TiO_2 films. *J. Photochem. Photobiol. A* **2006**, *182*, 43–51.

21. Lianjun, L.; Zhao, H.; Andino, J. M.; Li, Y. Photocatalytic CO_2 Reduction with H_2O on TiO_2 Nanocrystals: Comparison of Anatase, Rutile, and Brookite Polymorphs and Exploration of Surface Chemistry. *ACS Catal.* **2012**, *2*, 1817−1828.

22. Gordon, T. R.; Cargnello, M.; Paik, T.; Mangolini, F.; Weber, R. T.; Fornasiero, P.; Murray, C. B. Nonaqueous Synthesis of TiO_2 Nanocrystals Using TiF_4 to Engineer Morphology, Oxygen Vacancy Concentration, and Photocatalytic Activity. *J. Am. Chem. Soc.* **2012**, *134*, 6751−6761.

23. Dong, A.; Ye, X.; Chen, J.; Kang, Y.; Gordon, T.; Kikkawa, J. M.; Murray, C. B. A Generalized Ligand-Exchange Strategy Enabling Sequential Surface Functionalization of Colloidal Nanocrystals. *J. Am. Chem. Soc.* **2011**, *133*, 998–1006.

24. Downs, R. T.; Bartelmehs, K. L.; Gibbs, G. V.; Boisen, M. B. Interactive software for calculating and displaying X-ray or neutron powder diffractometer patterns of crystalline materials. *Am. Mineral.* **1993**, *78*, 1104-1107.

25. Buonsanti, R.; Grillo, V.; Carlino, E.; Giannini, C.; Kipp, T.; Cingolani, R.; Cozzoli, P. D. Nonhydrolytic Synthesis of High-Quality Anisotropically Shaped Brookite TiO_2 Nanocrystals. *J. Am. Chem. Soc.* **2008**, *130*, 11223-11233.